Fermi National Accelerator Laboratory

FERMILAB-Pub-93/064-E
E687

# Analysis of the Decay Mode $D^+ \to \overline{K}^{*0}\mu^+\upsilon$

P.L. Frabetti et al
The E687 Collaboration

*Fermi National Accelerator Laboratory*
*P.O. Box 500, Batavia, Illinois 60510*

April 1993

Submitted to *Physics Letters B*

Operated by Universities Research Association Inc. under Contract No. DE-AC02-76CHO3000 with the United States Department of Energy

## Disclaimer

# Analysis of the Decay Mode $D^+ \to \overline{K}^{*0}\mu^+\nu$

P.L. Frabetti
*Dip. di Fisica dell'Università and INFN - Bologna, I-40126 Bologna, Italy*

G.P. Grim, V.S. Paolone, P.M. Yager
*University of California-Davis, Davis, CA 95616 USA*

C.W. Bogart[a], H.W.K. Cheung, S. Culy, J.P. Cumalat, C. Dallapiccola, J.F. Ginkel, S.V. Greene, W.E. Johns, M.S. Nehring
*University of Colorado, Boulder, CO 80309, USA*

J.N. Butler, S. Cihangir, I. Gaines, P.H. Garbincius, L. Garren, S. Gourlay, D.J. Harding, P. Kasper, A. Kreymer, P. Lebrun, H. Mendez[b], S. Shukla
*Fermilab, Batavia, IL 60510, USA*

S. Bianco, F.L. Fabbri, S. Sarwar, A. Spallone, A. Zallo
*Laboratori Nazionali di Frascati dell'INFN, I-00044 Frascati, Italy*

R. Culbertson, R.W. Gardner, R. Greene, G. Jaross[c], K. Lingel[d], J. Wiss
*University of Illinois at Urbana-Champaign, Urbana, IL 61801, USA*

B.G. Cheon, J.S. Kang, K.Y. Kim
*Korea University, Seoul 136-701, Korea*

G. Alimonti, G. Bellini, B. Caccianiga, L. Cinquini, M. Di Corato, M. Giammarchi, P. Inzani, F. Leveraro, S. Malvezzi, D. Menasce, E. Meroni, L. Moroni, D. Pedrini, L. Perasso, A. Sala, S. Sala, D. Torretta[e], M. Vittone[e]
*Dip. di Fisica dell'Università and INFN - Milano, I-20133 Milan, Italy*

F. Davenport
*University of North Carolina-Asheville, Asheville, NC 28804 USA*

J.F. Filasetta
*Northern Kentucky University, Highland Heights, KY 41076 USA*

D. Buchholz, D. Claes[f], B. Gobbi, B. O'Reilly, S. Park[e], R. Yoshida[g]
*Northwestern University, Evanston, IL 60208, USA*

J.M. Bishop, J.K. Busenitz[h], N.M. Cason, J.D. Cunningham[i], C.J. Kennedy, G.N. Kim, T.F. Linn, E.J. Mannel[j], R.J. Mountain[k], D.L. Puseljic, R.C. Ruchti, W.D. Shephard, J.A. Swiatek, Z.W. Wu, M.E. Zanabria
*University of Notre Dame, Notre Dame, IN 46556, USA*

V. Arena, G. Boca, C. Castoldi, R. Diaferia, G. Gianini, S.P. Ratti, C. Riccardi, P. Vitulo
*Dip. di Fisica Nucleare dell'Università and INFN - Pavia, I-27100 Pavia, Italy*

A. Lopez
*University of Puerto Rico at Mayaguez, Puerto Rico*

J.R. Wilson
*University of South Carolina, Columbia, SC 29208 USA*

G.R. Blackett, M. Pisharody, T. Handler
*University of Tennesee, Knoxville, TN 37996 USA*

P.D. Sheldon
*Vanderbilt University, Nashville, TN 37235 USA*

Fermilab high-energy photoproduction experiment E687 provides a high statistics sample of the decay mode $D^+ \to \overline{K}^{*0}\mu^+\nu$ (charge conjugates are implied). Our analysis yields a branching ratio of $\Gamma(D^+ \to \overline{K}^{*0}\mu^+\nu)/\Gamma(D^+ \to K^-\pi^+\pi^+) = .56 \pm .04 \pm .06$. The ratios of the form factors governing the decay are measured to be $R_v = 1.74 \pm .27 \pm .28$ and $R_2 = .78 \pm .18 \pm .10$, implying a polarization of $\Gamma_l/\Gamma_t = 1.20 \pm .13 \pm .13$ for the electron decay. Finally, we report new limits on the decay modes $D^+ \to K^-\pi^+\mu^+\nu$ (nonresonant) and $D^+ \to \overline{K}^{*0}\pi^0\mu^+\nu$

We report on an analysis of a very clean sample of $875 \pm 44$ events of the decay mode $D^+ \rightarrow \overline{K}^{*0}\mu^+\nu$. The data were collected in the photoproduction experiment E687, conducted in the Fermilab Wideband Photon beam during the 1987-1988 and 1990-1991 fixed-target runs.

Several different models exist which predict the form factors for this decay and initial interest in this topic developed when the first experimental measurements appeared to disagree with the predictions [1].

The E687 detector[2] studies high-energy photon-Beryllium interactions using a multiparticle magnetic spectrometer with excellent vertex measurement, particle identification, and calorimetric capabilities. The average triggered photon energy is approximately 200 GeV. The trigger requires evidence of tracks outside the region where Bethe-Heitler pairs are produced and a minimum hadronic energy in our hadronic calorimeter. Charged particles emerging from the experimental target are tracked through a twelve-plane silicon microstrip vertex detector, an analysis magnet, three stations of multiwire proportional chambers, a second analysis magnet, and two more multiwire proportional chambers. The vertex detector measures decay proper times with approximately .048 ps resolution for charm particles which decay with all daughters detected in the microstrips. Three Čerenkov counters with different thresholds allow kaons to be separated from pions over a momentum range from 4.5 to 61 GeV/c. Particle tracks are projected through the inner electromagnetic calorimeter, hadron calorimeter, and additional shielding and are matched to hits in the inner muon detector consisting of three planes of scintillators and four planes of 5.08 cm diameter proportional tubes, covering approximately $\pm$ 40 mrad.

The data were reconstructed and then skimmed by requiring evidence of detached vertices in the event. Specifically, all high-quality two-track vertices were formed and the event was accepted if any two vertices were separated by more than $4.5\sigma$[3].

In this analysis, all tracks are searched for correct sign, mass, lepton and Čerenkov identification combinations to form $K\pi\mu$ candidates. All tracks must be found in the microstrips and the PWC system. The muon is identified in the inner muon detector where it must leave hits in at least three of the seven planes if the momentum is less than 30 GeV/c, and at least five of the seven planes if the momentum is greater than 30 GeV/c. The kaon must be identified by the Čerenkov system as kaon definite or kaon-proton ambiguous and the pion and muon must not be identified as a kaon or proton.

We require the $K\pi\mu$ combination to form a good vertex with a confidence level greater than 10%. The muon must have a momentum greater than 10 GeV/c and the $K\pi\mu$ combination must have a momentum greater than 50 GeV/c. Background from $D^+ \rightarrow K^-\pi^+\pi^+$, where a pion is misidentified as a muon, is eliminated by requiring

that the reconstructed $K\pi\mu$ mass be less than 1.8 GeV/c$^2$.

The primary tool for eliminating non-charm backgrounds is to require a statistically significant detachment of the secondary vertex from the primary production vertex. We find the primary vertex by searching for the most upstream high-quality vertex in the target region that can be made from the tracks which remain after the $K\pi\mu$ combination is removed. The distance between the primary and secondary vertices is $\ell$ and its measurement error is $\sigma$. We require detachment by cutting on the normalized separation between the primary and secondary vertices, $\ell/\sigma$.

Finally, we require that the $K\pi\mu$ vertex be isolated from other tracks in the event (not including tracks in the primary vertex) by requiring that the maximum confidence level for another track to form a vertex with the candidate be less than 1%.

Figure 1a shows the $K\pi$ invariant mass distribution for right-sign ($Q_K + Q_\mu = 0$) and wrong-sign ($Q_K + Q_\mu \neq 0$) candidates which pass all cuts and have a detachment $\ell/\sigma > 20$. The $K^-\pi^+$ mass right-sign signal is dominated by the $\overline{K}^{*0}(892)$.

The $K^-\pi^+\pi^+$ signal used for the branching ratio normalization is found with the same skim requirements, vertexing scheme, and cuts, except for the muon cuts. The resulting signal[4] is shown in Figure 1b.

Figure 2 shows the wrong-sign subtracted signals for several $\ell/\sigma$ cuts. Note that the low mass bump from the decay $D^{*+} \to (K^-\mu^+\nu)\pi^+$ disappears with larger detachment cuts due to the shorter $D^0$ lifetime. We use the sample with $\ell/\sigma > 20$ for all reported results.

Because of the undetected neutrino, we cannot fully reconstruct the $D^+$ invariant mass and therefore we are open to contamination from other partially reconstructed charm decays which include a $\overline{K}^{*0}$. Figure 3a shows the signal's survival *vs* the $\ell/\sigma$ cut compared to the survival predicted by our $D^+$ Monte Carlo. The very good agreement at longer detachments indicates little contamination from shorter lived charm states beyond $\ell/\sigma > 5$.

Figure 3b shows the signal survival as a function of the minimal confidence level requirement for the secondary vertex compared to that predicted by our Monte Carlo. The accumulation of events at low secondary vertex confidence level in the data suggests there is some contamination from charm backgrounds where the $K\pi\mu$ tracks do not originate from a common vertex. Most of this background is eliminated by the requirement that the secondary vertex confidence level exceeds 10%.

Figure 3c compares the data and Monte Carlo response to the secondary vertex

isolation cut. Here the vertex is more isolated as the confidence level cut gets smaller. Agreement is good indicating negligible potential background from charm states with an additional charged track in the same vertex as the $K\pi\mu$ candidate. We require this confidence level to be less than 1%.

We are left with a potential background from $D^+ \to \overline{K}^{*0}\pi^0\mu\nu$ decay where an undetected $\pi^0$ accompanies the $K^-\pi^+\mu^+$ tracks. If our data were to include a substantial $\overline{K}^{*0}\pi^0\mu\nu$ contamination, one would expect the observed average $K^-\pi^+\mu^+$ mass to be lower than the Monte Carlo prediction. We find that average $K^-\pi^+\mu^+$ invariant mass observed in our signal is $1.373 \pm .006$ Gev/c$^2$ which is in good agreement with the Monte Carlo prediction of 1.379 Gev/c$^2$ obtained using our measurement of the form factors.

To put a quantitative limit on contamination, we fit the two dimensional distribution of the $K^-\pi^+$ mass and the $K^-\pi^+\mu^+$ mass. The fit function is a combination of the Monte Carlo distributions for the signal, $D^+ \to (K^-\pi^+)\mu^+\nu$, the nonresonant decay $D^+ \to K^-\pi^+\mu^+\nu$, the background from $D^{*+} \to (K^-\mu^+\nu)\pi^+$, and the contaminations $D^+ \to (K^-\pi^+)\pi^0\mu^+\nu$ and $D^+ \to (K^-\pi^0)\pi^+\mu^+\nu$. The fit is performed under the constraint that the last two modes follow from the decay of an I=1/2 resonance[5]. The fit results give:

$$\frac{\Gamma(D^+ \to K^-\pi^+\mu^+\nu(\text{nonresonant}))}{\Gamma(D^+ \to (K^-\pi^+)\mu^+\nu)} = .083 \pm .029$$

or a limit of $< .12$ at the 90% confidence level and:

$$\frac{\Gamma(D^+ \to (K^-\pi^+)\pi^0\mu^+\nu)}{\Gamma(D^+ \to (K^-\pi^+)\mu^+\nu)} < .042$$

at the 90% confidence level.

We now present a new measurement of $\Gamma(D^+ \to \overline{K}^{*0}\mu^+\nu)/\Gamma(D^+ \to K^-\pi^+\pi^+)$[4]. Background from $\overline{K}^{*0}\pi^+\pi^0$ where the pion is misidentified as a muon is corrected for by assuming a 1.3% misidentification probability which we measure with high statistics charm decays.

Possible contamination from $\overline{K}^{*0}\pi^0\mu\nu$ is included as a systematic together with signal fitting, nuclear scattering, and uncertainty in triggering energy. The result is $\Gamma(D^+ \to \overline{K}^{*0}\mu\nu)/\Gamma(D^+ \to K^-\pi^+\pi^+) = .56 \pm .04 \pm .06$. This ratio includes a correction factor for the undetected decay $\overline{K}^{*0} \to \overline{K}^0\pi^0$. The current world average (measured using the equivalent electron decay mode) is $.51 \pm .05$[6].

To fit for the form factors, we use the matrix element form and methodology found in [1] and calculate the kinematic variables, $\cos\theta_v$, the angle between the $\pi$

and the $D$ direction in the $\overline{K}^{*0}$ rest frame, $\cos\theta_l$, the angle between the $\nu$ and the $D$ direction in the $\mu\nu$ rest frame, and $t$, the square of the $\mu\nu$ mass. $D^-$ decays have the same definition of variables and no change is required in the matrix element. We integrate over the fourth kinematic variable, the coplanarity angle, because it provides no significant information on the form factors. We assume that the reconstructed $D$ momentum vector points along the line defined by the primary and secondary vertex. This leaves a two-fold ambiguity and we use the solution that gives the lower $D$ momentum which yielded slightly better estimates for the kinematic variables in Monte Carlo studies.

Due to resolution, 50% of events are reconstructed outside physical limits (the $p_\perp$ of the charged daughters relative to the $D^+$ direction implies the decay of a particle with a mass larger than the $D^+$ mass). These events are recovered by moving the primary vertex to the nearest allowed solution and the kinematic variables are recomputed. Monte Carlo studies show that the inclusion of the recovered events does not significantly degrade the resolution. The resolution in the kinematic variables, including the effects of the ambiguity and recovery, is small compared to the structure of the distributions we are measuring. We find that requiring that the reconstructed event be physical or nearly physical does not significantly improve signal to noise.

We use a binned maximum likelihood fit to determine the form factors. We bin the sample into three equal bins in $\cos\theta_v$, three in $\cos\theta_l$, and two in $t/t_{max}$. In the absence of lepton mass effects, there are two axial and one vector form factor, $A_1(t)$, $A_2(t)$, and $V(t)$. We assume these form factors have a simple pole dependence with masses $M_A = 2.5$ GeV and $M_V = 2.1$ GeV[1], and fit for the ratio of the form factors evaluated at $t = 0$: $R_v = V(0)/A_1(0)$ and $R_2 = A_2(0)/A_1(0)$.

In the fit, the prediction of the yield in each bin is the integral of the matrix element over the bin. This number is multiplied by a Monte Carlo correction factor which is the number of events reconstructed in the bin divided by the number generated in the bin with a trial set of form factors. The correction is largest at low $\cos\theta_l$ and low $t$, where the efficiency is approximately half the maximum efficiency. Because of finite bin size and resolution, the Monte Carlo correction depends on the form factors so we take the current fit results, recalculate the correction, and perform the fit again. We find that only two iterations are necessary.

To predict the background in a right-sign bin, we add the wrong-sign yield in the bin, scaled by a third fit parameter, the background level. This fit parameter allows background level fluctuations to be reflected in the form factor errors, and it is tied to the observed number of wrong-sign events through an additional Poisson factor in the likelihood.

This fit procedure eliminates any biases from events where the wrong solution is

chosen, recovered unphysical events, and resolution. It has the advantage that we are not required to invent a background parameterization[8]. Because the matrix element varies gradually over the three kinematic variables, one suffers only a slight ($< 20\%$) increase in the statistical error compared to a continuous likelihood fit with a parameterized background.

The correction due to finite muon mass is done in two stages. The matrix element in the fit function includes an overall factor of $(1 - M_\mu^2/t)^2$. The (much smaller) additional finite mass terms are included in the Monte Carlo correction factors on successive iterations. We assume that the third form factor in the finite mass terms, $R_3$, is zero. To assess our sensitivity to this assumption, we fit for $R_v$ and $R_2$ in Monte Carlo samples generated with $R_3 = 0$ and $R_3 = 3$ and found the results varied by less than 7% of our statistical error.

Figure 4 compares the actual bin populations observed in the data with the yield predicted by the form factor fit. The first 9 bins are $t/t_{max} < .5$. Of these, the first three are for the lowest value of $\cos\theta_l$ and are increasing in $\cos\theta_v$, *etc.* The fit results are: $R_v = 1.74 \pm .27 \pm .28$, $R_2 = .78 \pm .18 \pm .10$. $R_v$ and $R_2$ are correlated by -15%. To facilitate comparisons to other measurements, we report the polarization for the electron decay, *i.e.* we set the lepton mass to the mass of the electron and integrate over the appropriate parts of the matrix element. The polarization for these values of $R_v$ and $R_2$ is $\Gamma_l/\Gamma_t = 1.20 \pm .13 \pm .13$.

The dominant systematic error was conservatively estimated from the change in the fit result when the wrong-sign background is increased by 50%. The systematic error also includes the possibility of local variations in the muon identification efficiency, and uncertainty in the triggering energy.

To summarize the results, we have measured the branching ratio $\Gamma(D^+ \to \overline{K}^{*0}\mu^+\nu)/\Gamma(D^+ \to K^-\pi^+\pi^+) = .56 \pm .04 \pm .06$. We compare our measurement of the form factors in the semileptonic decay $D^+ \to \overline{K}^{*0}\mu^+\nu$ to other recent measurements of the form factors in Table I.

We wish to acknowledge the assistance of the staffs of Fermilab, the physics departments of the University of Colorado, the University of Illinois, Northwestern University, and the University of Notre Dame, and the I.N.F.N. Sections and the Physics departments of the Bologna University, Milano University, and Pavia University. This research was supported in part by the National Science Foundation, the U.S. Department of Energy, the Italian Istituto Nazionale di Fisica Nucleare and Ministero dell'Università e della Ricerca Scientifica.

## REFERENCES


[a] Present address: Vector Research Company, 6903 Rockledge Drive, Bethesda, MD 20817, USA.

[b] Present address: Cinvestav-IPN, A.P. 14-740, 07000 Mexico DF, Mexico.

[c] Present address: STX Inc.,4400 Forbes Blvd., Lanham, MD 20706, USA.

[d] Present address: University of Colorado, Boulder, CO 80309, USA.

[e] Present address: Fermilab, Batavia, IL 60510, USA.

[f] Present address: University of New York, Stony Brook, NY 11794, USA.

[g] Present address: NIKHEF-H, 1009 DB, Amsterdam, The Netherlands.

[h] Present address: University of Alabama, Tuscaloosa, AL 35487, USA.

[i] Present address: Brandeis University, Waltham, MA 02254, USA.

[j] Present address: Nevis Labs, Columbia University, Irvington, NY 10533, USA.

[k] Present address: Syracuse University, Syracuse, NY 13244-1130 USA.



[1] E691 Collab., J. C. Anjos et al., Phys. Rev. Lett. 65 (1990) 2630.

[2] E687 Collab., P. L. Frabetti et al., Nucl. Instrum. Methods. A320 (1992) 519.

[3] Approximately 9% of data (from the early 1987-1988 run) were skimmed with a $3\sigma$ requirement.

[4] For Figure 1b and for the branching ratio $\Gamma(D^+ \to \overline{K}^{*0}\mu^+\nu)/\Gamma(D^+ \to K^-\pi^+\pi^+)$ we rejected approximately 45% of the data. In 1991 our inner muon system was reconfigured to accommodate a downstream experiment and the additional noise caused unacceptable systematics for the branching ratio measurement. The form factor analysis is much less sensitive to this so we include the full data sample in that analysis and in Figure 1a.

[5] E691 Collab., J. C. Anjos et al., Phys. Rev. D 45 (1992) R2177.

[6] Particle Data Group, K. Hikasa et al., Phys. Rev. D 45 S1 (1993).

[7] J.G. Korner and G.A. Schuler, Z. Phys. C 46 (1990) 93.

[8] However the effects of additional fluctuations in the fit parameters due to resolution smearing and background shape fluctuation are not included in the returned fit errors. We have therefore multiplied all quoted errors by a factor of 1.14 based on a Monte Carlo study where fits were made to many simulated data sets including simulated background.

[9] E653 Collab., K. Kodama et al., Phys. Lett. B 274 (1992) 246.

## TABLES

TABLE I. Form Factor Measurements

| | $R_v$ | $R_2$ | $\Gamma_l/\Gamma_t$ |
|---|---|---|---|
| This paper | $1.74 \pm .27 \pm .28$ | $.78 \pm .18 \pm .10$ | $1.20 \pm .13 \pm .13$ |
| E691[1] | $2.0 \pm .6 \pm .3$ | $0.0 \pm .5 \pm .2$ | $1.8 \, ^{+.6}_{-.4} \pm .13$ |
| E653[9] | $2.00 \, ^{+.34}_{-.32} \pm .16$ | $.82 \, ^{+.22}_{-.23} \pm .11$ | $1.18 \pm .18 \pm .08$ |

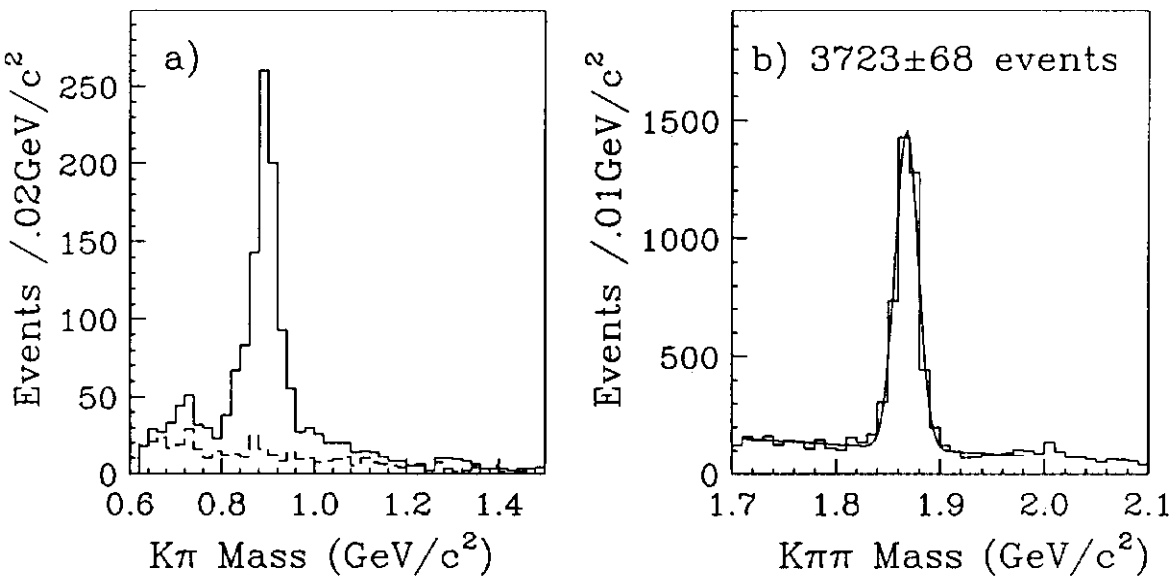


FIG. 1. The a) $K^-\pi^+$ mass for right-sign (solid) and wrong-sign (dashed) $D^+ \to \overline{K}^{*0}\mu^+\nu$ candidates with $\ell/\sigma > 20$ and b) $K^-\pi^+\pi^+$ mass for $D^+ \to K^-\pi^+\pi^+$ candidates. The solid line is a fit to the distribution.

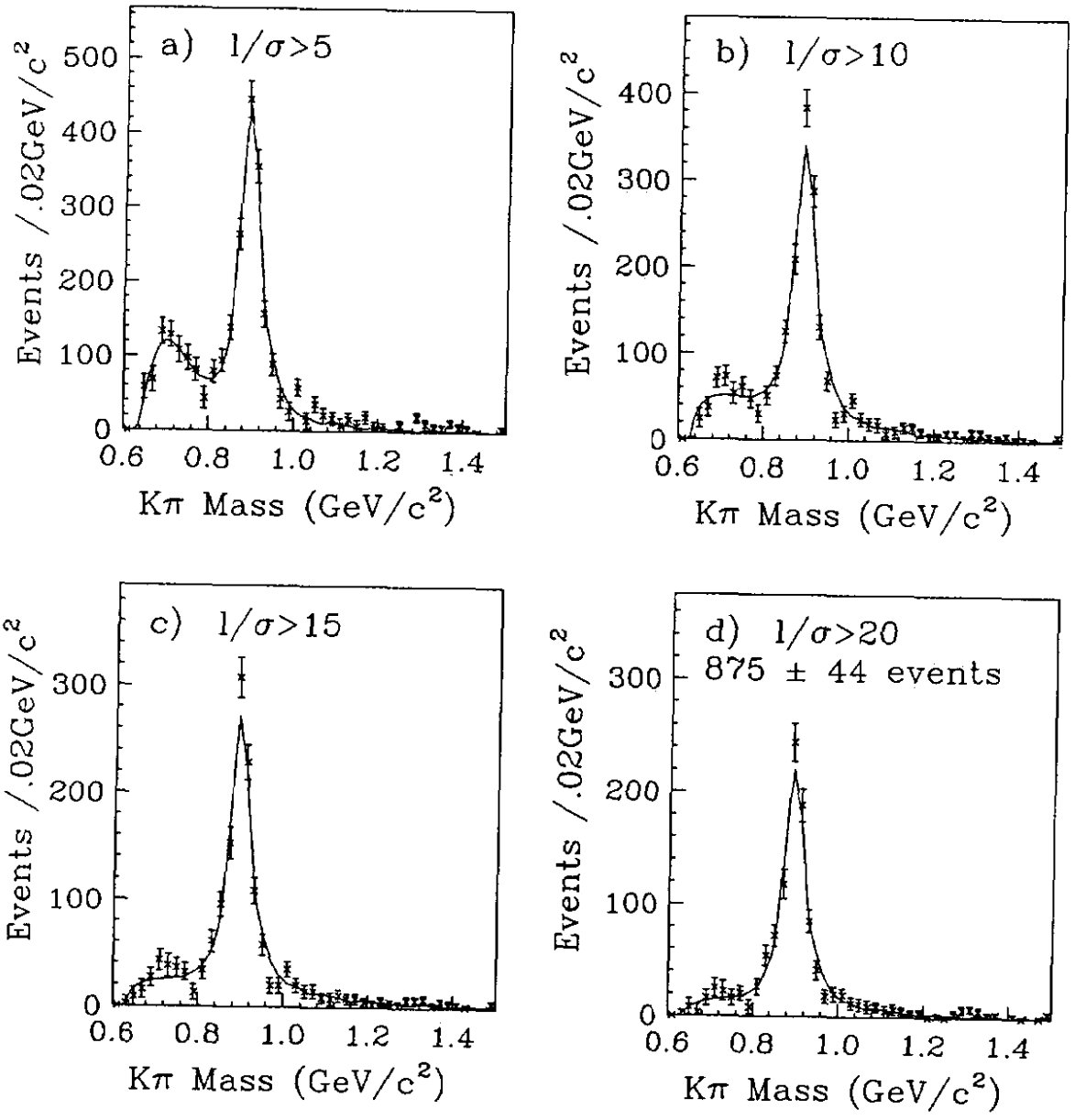


FIG. 2. The $K^-\pi^+$ mass after wrong-sign subtraction for $D^+ \to \overline{K}^{*0}\mu^+\nu$ candidates with secondary vertex separation cuts a) $\ell/\sigma > 5$, b) $\ell/\sigma > 10$, c) $\ell/\sigma > 15$, and d) $\ell/\sigma > 20$. Fits are shown as solid lines.

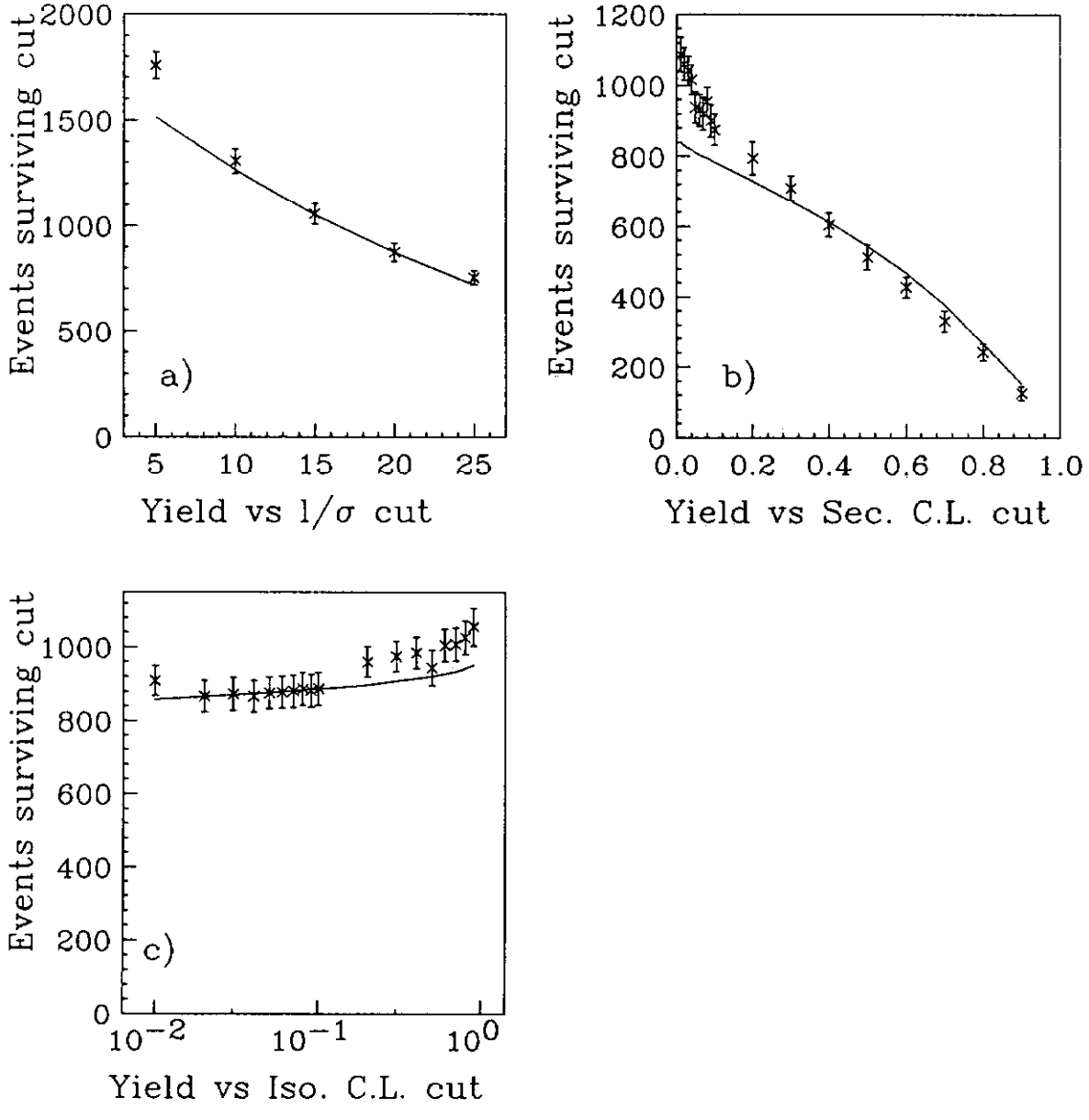


FIG. 3. Yields for $D^+ \to \overline{K}^{*0}\mu^+\nu$ as a function of a) the $\ell/\sigma$ cut, b) the secondary vertex confidence level cut, and c) the secondary vertex isolation confidence level cut. The Monte Carlo predictions are shown as solid lines.

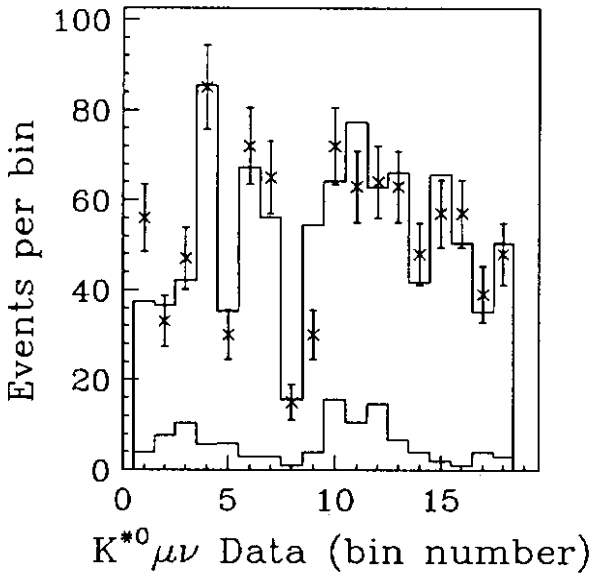


FIG. 4. The form factor fit displayed in the 18 bins (see text). The bin populations for the data are shown as the points with error bars. The upper histogram shows the sum of the bin populations expected for our measured form factors and the wrong-sign background bin populations (shown in the lower histogram).